5th International Conference on Energy Sustainability
ASME
August 7-10, 2011, Grand Hyatt Washington, Washington DC, USA

ESFuelCell2011-54254

# HEAT LOSS CHARACTERISTICS OF A ROOF INTEGRATED SOLAR MICRO-CONCENTRATING COLLECTOR

**Tanzeen Sultana**
University of New South Wales
Kensington, NSW, Australia

**Graham L Morrison**
University of New South Wales
Kensington, NSW, Australia

**Siddarth Bhardwaj**
University of New South Wales
Kensington, NSW, Australia

**Gary Rosengarten**
University of New South Wales
Kensington, NSW, Australia

## ABSTRACT

Concentrating solar thermal systems offer a promising method for large scale solar energy collection. It is feasible to use concentrating solar thermal systems for rooftop applications such as domestic hot water, industrial process heat and solar air conditioning for commercial, industrial and institutional buildings. This paper describes the thermal performance of a new low-cost solar thermal micro-concentrating collector (MCT), which uses linear Fresnel reflector technology and is designed to operate at temperatures up to 220°C. The modules of this collector system are approximately 3 meters long by 1 meter wide and 0.3 meters high. The objective of the study is to optimize the design to maximise the overall thermal efficiency. The absorber is contained in a sealed enclosure to minimise convective losses. The main heat losses are due to natural convection inside the enclosure and radiation heat transfer from the absorber tube. In this paper we present the results of a computational investigation of radiation and convection heat transfer in order to understand the heat loss mechanisms. A computational model for the prototype collector has been developed using ANSYS-CFX, a commercial computational fluid dynamics software package. Radiation and convection heat loss has been investigated as a function of absorber temperature. Preliminary ray trace simulation has been performed using SolTRACE and optical efficiency has been evaluated. Finally, the MCT collector efficiency is also evaluated.

## INTRODUCTION

In recent years, many non-concentrating roof-integrated collectors have been proposed, such as hybrid systems with photovoltaic or thermoelectric elements [1]. Rooftop integrated concentrating solar thermal systems are not common and only a few projects are mentioned in the

literature [2-5]. Until now, the commercially available high temperature solar thermal technologies such as parabolic trough and linear Fresnel, have not integrated well on rooftops as they have been complex, cumbersome, have high wind loading and are difficult to maintain.

In this paper, a new low-cost micro-concentrator collector (MCT) has been studied, which is designed to operate at temperatures up to 220°C, and be seamlessly integrated into the architecture of buildings. The applications of this system include domestic hot water, industrial process heat and solar air conditioning for commercial, industrial and institutional buildings (Figure 1).

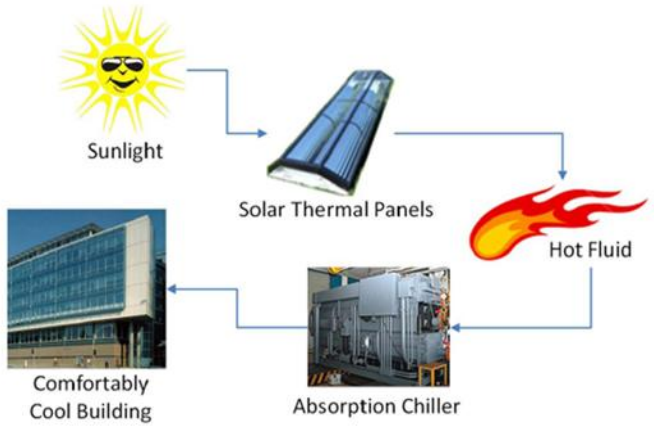


Figure 1: Example of concentrating panel solar cooling schematic.

Rooftop solar cooling technologies need to be very space efficient. As low temperatures can only be used to drive single effect chillers, traditional flat panel collectors need more than twice the roof area to produce sufficient cooling for a low rise building. High temperature systems, such as parabolic trough collectors, require more space on the rooftop to avoid shading as they track the sun. In this regard the MCT is considered more efficient compared to both low temperature collectors and more complex high temperature systems [2].

### Description of MCT Collector

The MCT system module is approximately 3.2 meters long by 1.2 meters wide and 0.3 meters high (Figure 2). As illustrated in Figure 3, the MCT collector utilizes linear Fresnel reflector optics. The Fresnel reflectors concentrate beam radiation to a stationary receiver. The receiver consists of two 16 mm diameter stainless steel absorber tubes. Each receiver has a secondary reflector that directs beam radiation to the absorber tube. The entire optic system is enclosed in a sealed glazed canopy. The basic design of the receiver area is illustrated in Figure 4.

Figure 2: A solar micro-concentrator system [6]

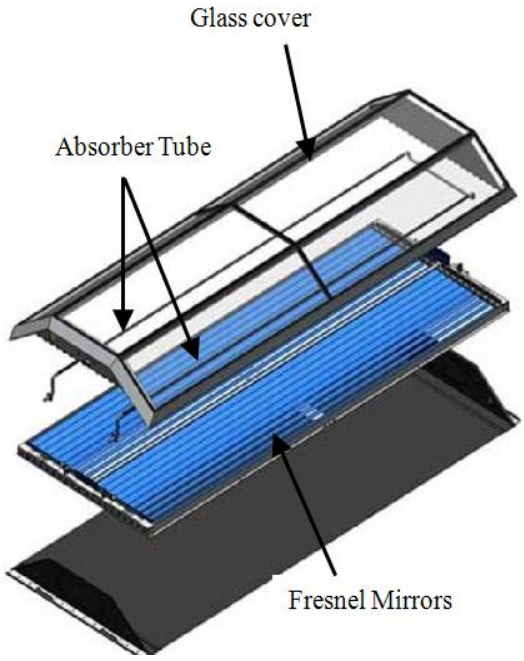


Figure 3: A solar micro-concentrator system [6]

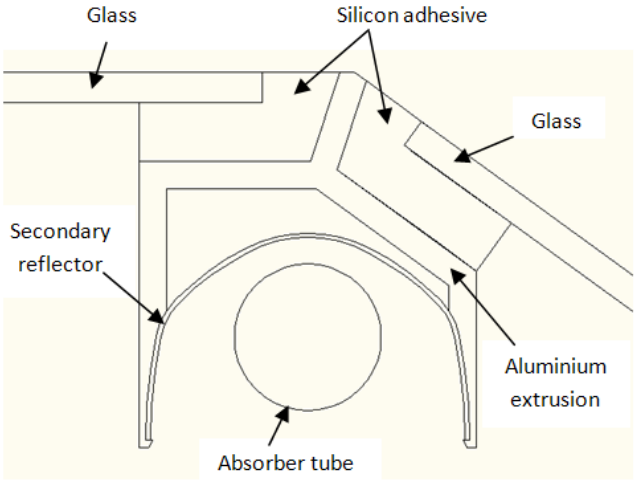


Figure 4: Receiver area of micro-concentrating collector

### Heat Loss of MCT Collector

Evaluation of heat losses from the receiver is an important input to the performance evaluation of the solar collector. To achieve high efficiency in a concentrating solar collector, there should be minimum thermal losses from the absorber. Figure 5 shows a schematic of the cavity along with the internal modes of heat transfer.

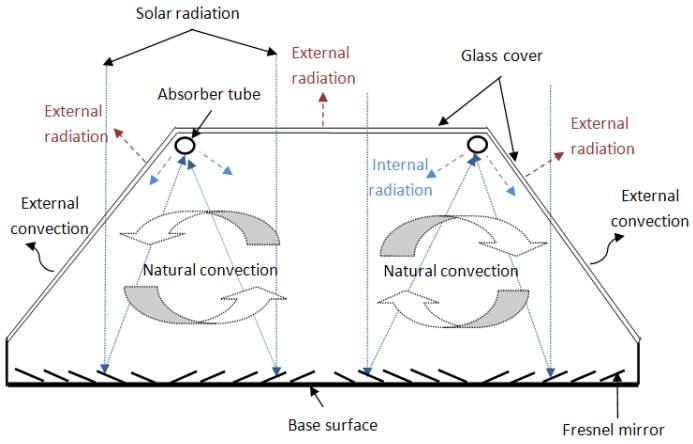


Figure 5: Cross-section of the micro-concentrating collector showing modes of internal heat transfer.

During operation, the hot absorber tube emits long-wavelength radiation into the cavity that is absorbed mainly by the bottom wall, which in turn heats up. This promotes buoyancy-driven flows within the cavity, resulting in convection losses and a further reduction in thermal efficiency [7].

The current study investigates the role of radiation and natural convection heat transfer inside the cavity, along with heat transfer at the boundaries in order to fully understand the heat loss mechanisms.

## NOMENCLATURE

$T_a$ = Ambient temperature ($^oC$)
$T_{abs}$ = Absorber temperature ($^oC$)
$\varepsilon_{abs}$ = Emissivity of absorber tube
G = Solar radiation intensity ($W/m^2$)
k = Thermal conductivity (W/m K)
W/m = Units in watts per meter length
D = Diameter of absorber tube

## COMPUTATIONAL MODELING

A computational model of the prototype absorber has been developed using ANSYS-CFX [8]. For simplicity, a two dimensional geometry with a symmetry plane is created (Figures 6-7) assuming the collector is mounted flat on a roof. The boundary conditions are as shown in Table 1.

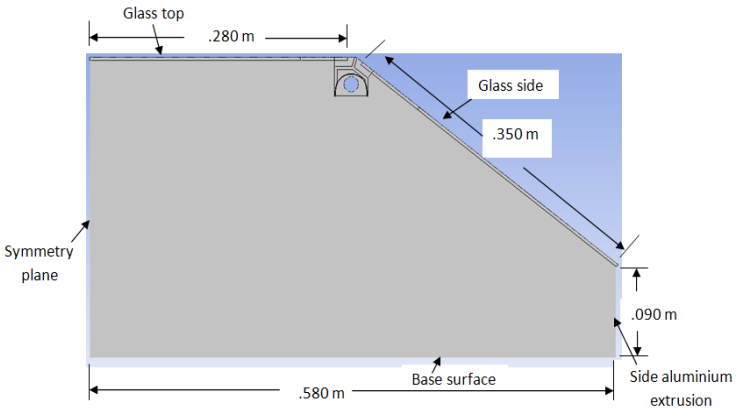


Figure 6: Cavity geometry for CFD modeling

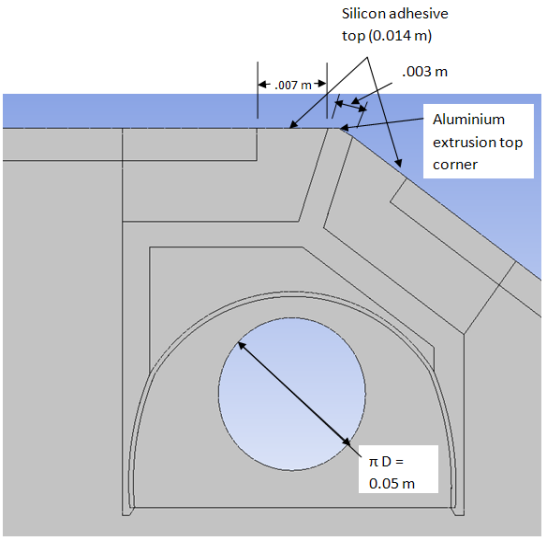


Figure 7: Receiver section geometry for CFD modeling

Table 1: Boundary Conditions for CFD

| | **Convective heat loss coefficient ($W/m^2$ K)** | **Emissivity** |
|---|---|---|
| Aluminium extrusion top corner | 10 | 0.05 |
| Silicon adhesive top | 10 | 0.9 |
| Glass cover | 10 | 0.9 |
| Base surface | 5 | 0.05 |
| Side aluminium extrusion | 5 | 0.05 |
| Absorber tube | | 0.05 |

The absorber tube is modelled as an isothermal surface. The convective flow and resulting temperature distribution between the absorber tube and the secondary reflector and glass cover are studied for various absorber temperatures, from 100°C to 450°C. The absorber tube is coated with a selective surface, and the long wavelength emissivity is taken as 0.05. The cover glass at the top and sides of the cavity are modelled as convection boundaries with external heat loss coefficients of 10 $W/m^2K$, exchanging heat with an ambient temperature of 20°C. The glass has an internal emissivity of 0.9. The base of the cavity and aluminium side walls are also modeled as convection boundaries with external heat loss coefficients of 5 $W/m^2K$, exchanging heat with an ambient temperature of 20°C. The base reflector surface and aluminium side walls have an internal emissivity of 0.05.

The air flow in the cavity is modelled as laminar as the Rayleigh number is in the range of $1.8 \times 10^4$ - $2.7 \times 10^7$. Radiation is modelled using the Monte Carlo simulation method [9]. All discretization is carried out using second order schemes. Air properties are calculated using an ideal gas model. Minimum convergence criteria were set at $10^{-3}$ for continuity and velocity, and $10^{-6}$ for energy. A hybrid mesh is used with structured quadrilateral elements in the wall zones and unstructured triangular elements in the central zone of the collector cavity. The resulting mesh size is approximately 3 mm, with 60,000 mesh points in total. A grid dependency study has been undertaken to ensure the adequacy of this mesh density.

## Computational Results

The natural convection and radiation heat losses from the cavity receiver are determined for absorber temperatures from 100°C to 450°C. The air flow patterns in the receiver cavity of the collector are shown in Figure 8. Locations where fluid motion is fastest are along the glass side walls, and along the top surface. The next fastest fluid motion is a layer along the upper glass cover, with the fluid dropping down into the cavity from the glass at the symmetry plane. Although the bottom convective cells cover most of the cavity they do not significantly effect convection around the absorber.

For the boundary conditions specified in Table 1, the results show significant thermal gradients in the cavity only around the absorber and secondary reflector (Figures 9-10). Rising fluid around the absorber tube is entrapped by the secondary reflector thus reducing the convective heat loss from the absorber tube to the cavity (Figures 11-12).

In this study the secondary reflector around the absorber tube was considered to be a thin aluminum sheet. It may be possible to reduce the strength of the upper convection cell by using an insulated reflector.

Heat loss from different boundary zones are shown in Table 2. Due to the low emissivity of the absorber selective coating the radiation heat loss is only 15% to 20% of the convective heat loss (Figure 13). The heat loss coefficient from the absorber tube is calculated as 5.8 $W/m^2$ K. The total heat loss at 220°C is approximately 60W per meter length of tube compared to an expected solar input of approximately 300W to 400W per meter length.

The heat loss distribution over the external boundaries of the collector is shown in Figure 14. The results show a peak in the heat transfer above the absorber due partly to conduction through the aluminium support. To determine the effect of the aluminium support we carried out a parametric study on the support component thermal conductivity. The maximum boundary heat flux and the total heat loss decreases by approximately 20% if a low thermal conductivity support is used (Figure 15 and Table 3).

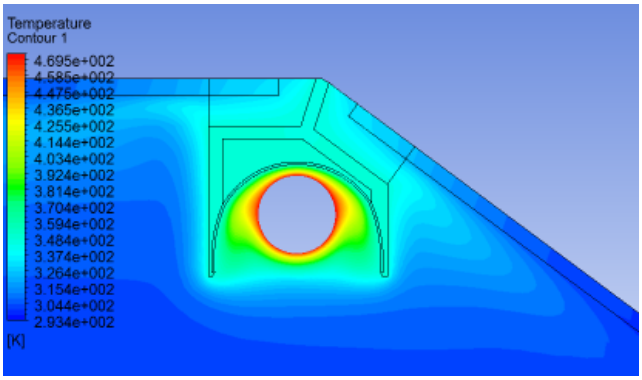


Figure 10: Temperature contours near the receiver (absorber tube temperature 200°C)

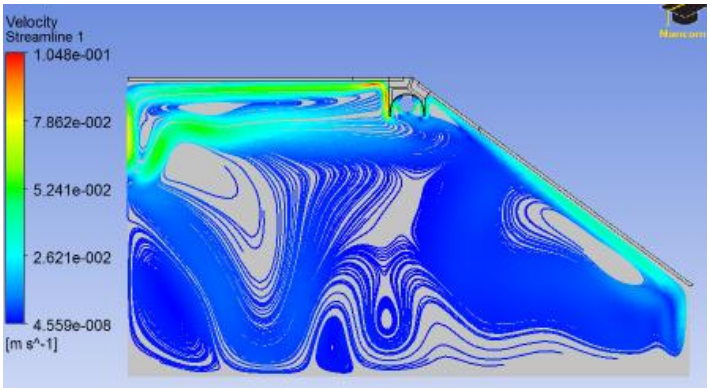


Figure 8: Velocity streamlines in the receiver cavity (absorber tube temperature 200°C)

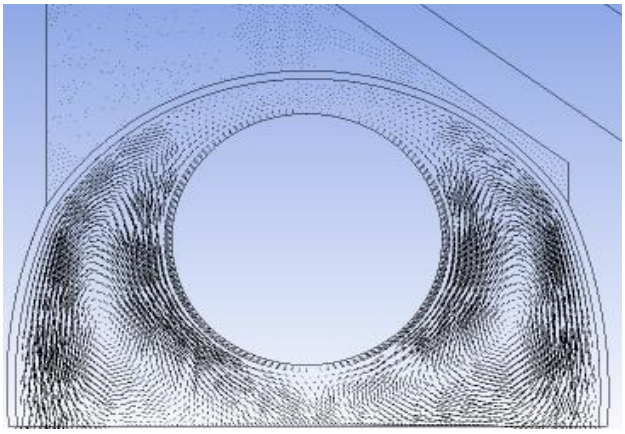

Figure 11: Velocity magnitude between absorber tube and secondary reflector (absorber tube temperature 200°C)

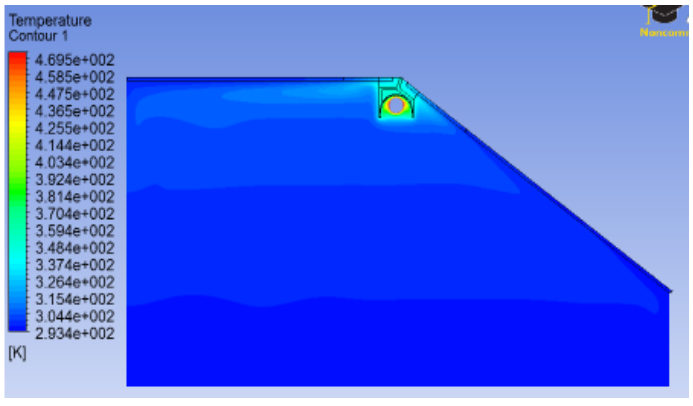


Figure 9: Temperature contours in the cavity receiver (absorber tube temperature 200°C)

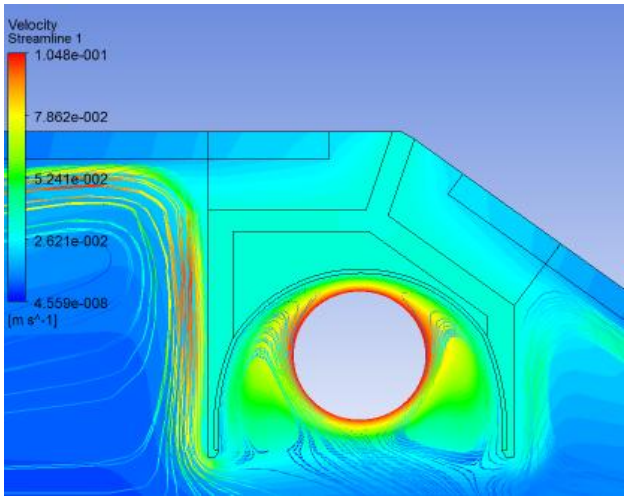


Figure 12: Streamlines near the receiver section (absorber tube temperature 200°C)

Table 2: Heat loss for 200°C absorber tube temperature

| | Heat loss (W/m) |
|---|---|
| Absorber tube | 58 |
| Glass top cover | 25 |
| Glass side cover | 23 |
| Base surface | 2 |
| Side aluminium extrusion | 1 |
| Aluminium extrusion top corner | 2 |
| Silicon adhesive top | 6 |

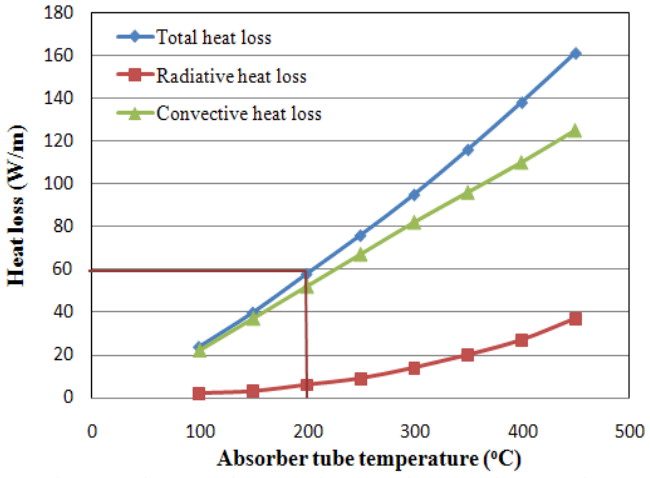


Figure 13: Absorber heat loss for different absorber temperatures

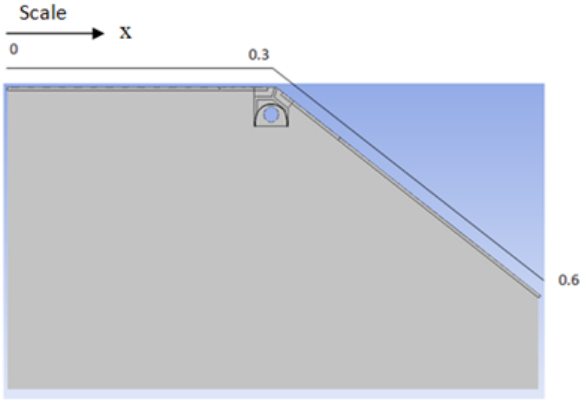


Figure 14 (a)

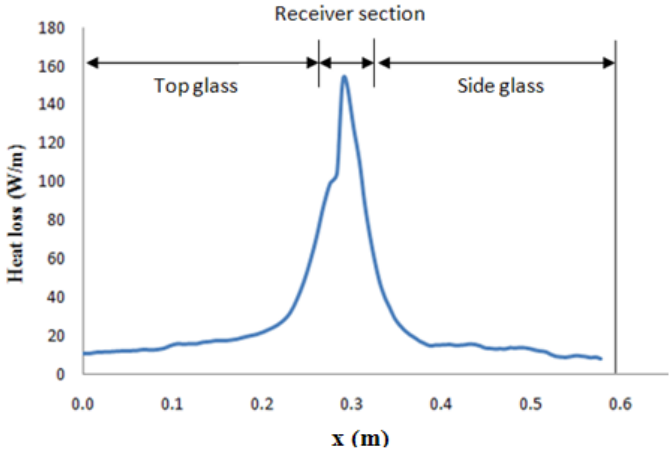


Figure 14 (b)

Figure 14: (a) Receiver cavity showing dimensions of external boundaries (b) Heat loss distribution overthe external boundary.

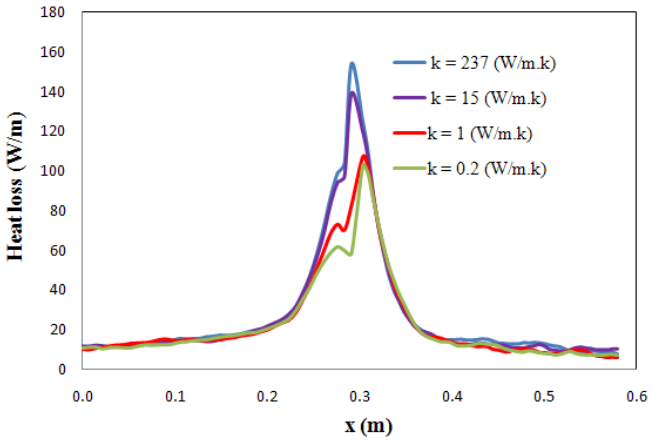


Figure 15: Heat loss distribution over the external boundary for different thermal conductivity of support component

Table 3: Heat loss from the absorber tube for different thermal conductivities of the support component

| Thermal conductivity (W/m K) of support component | Heat loss (W/m) of absorber tube |
|---|---|
| 237 (Aluminium) | 58 |
| 15 (Stainless steel) | 57 |
| 1 ( Glass) | 52 |
| 0.2 (Fibre) | 48 |

## OPTICAL PERFORMANCE

Raytrace analysis of the collector optics was carried out using the program SolTRACE [10] for the following material parameters.

Transmissivity of glass cover = 94 % ( non-varying with incdence angle)
Reflectance of primary (Fresnel) reflector =95 %
Reflectance of secondary reflector = 100% (not modelled)
Absorptance of absorber tube = 95%

The absorber tube and secondary reflector were simplified to a flat absorber of the same width as the secondary reflector aperture for ray trace modelling (Figure 16). Total radiation flux on the absorber surface for various incident angles are illustrated in Figure 17.

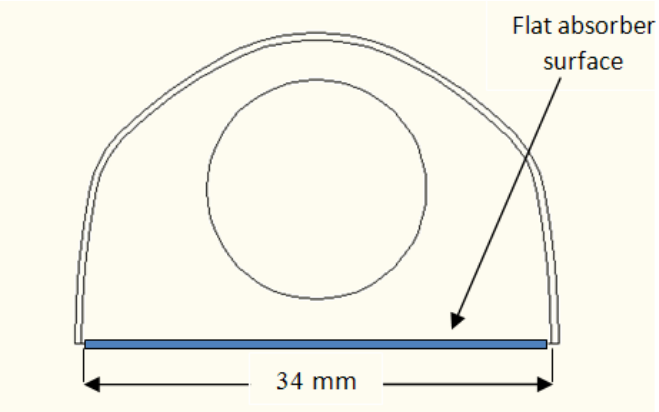


Figure 16: Flat absorber surface for simplified ray trace simulation

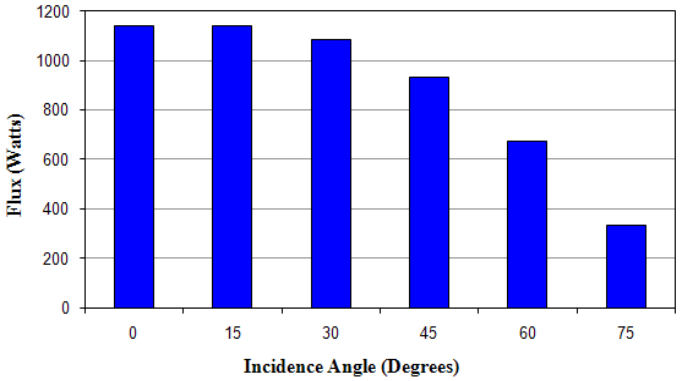


Figure 17: Total flux on each absorber tube for various incident angles for beam radiation = 1000 W/m$^2$

Three different measures of optical efficiency are shown in Figure 18 and calculated as follows:

$$\text{Efficiency} = \frac{\text{Flux on flat absorber}}{\text{Direct normal irradiation} \times \text{Aperture area}}$$

$$\text{Design Efficiency} = \frac{\text{Flux on flat absorber}}{\text{Direct normal irradiation} \times \text{Aperture area} \times \cos(\text{incidence angle})}$$

Geometric Efficiency = Design efficiency ignoring absorption/reflectance/transmission losses

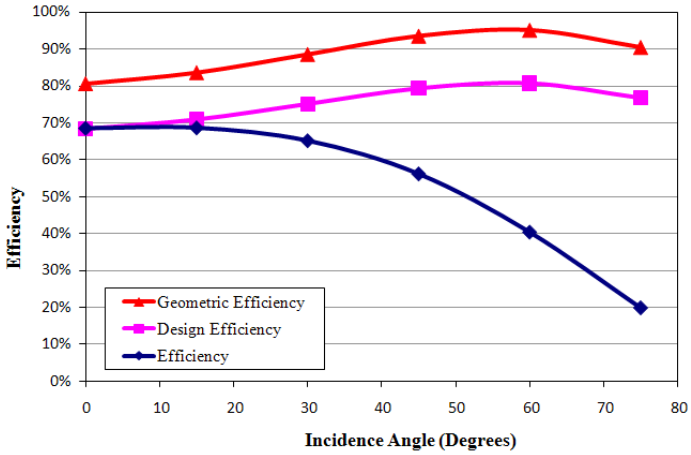


Figure 18: Optical efficiency as a function of incident angle

The main optical losses of the Fresnel reflector are shown in Figure 19. These effects can be reduced by making the collector deeper and by widening the gap between Fresnel mirror elements. On the other hand geometric changes cause losses due to inaccuracy of assembly and tracking of the primary mirrors. Further analysis will be carried

out to evaluate performance-related factors such as incidence angle modifiers and shading losses.

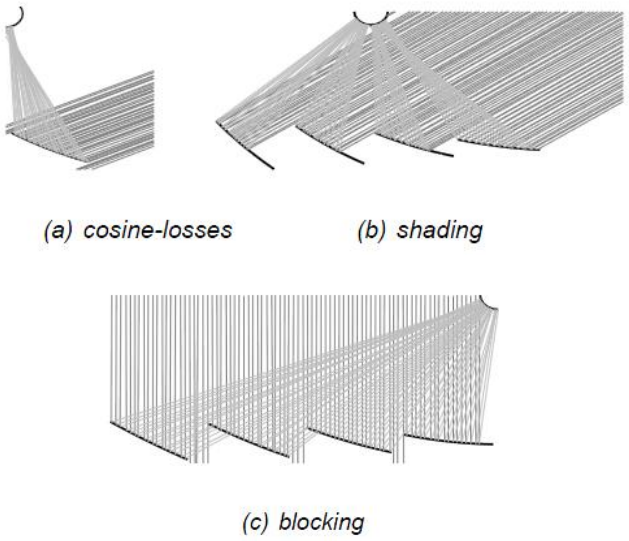


Figure 19: Geometry losses of Fresnel reflector

## MCT THERMAL EFFICIENCY

The MCT thermal efficiency characteristic was determined by combining the calculated optical efficiency and heat loss as plotted in Figure 20. Solar beam radiation is taken as G = 1000 W/m$^2$. The MCT system shows an efficiency of 60% at its design operating temperature of 200$^o$C.

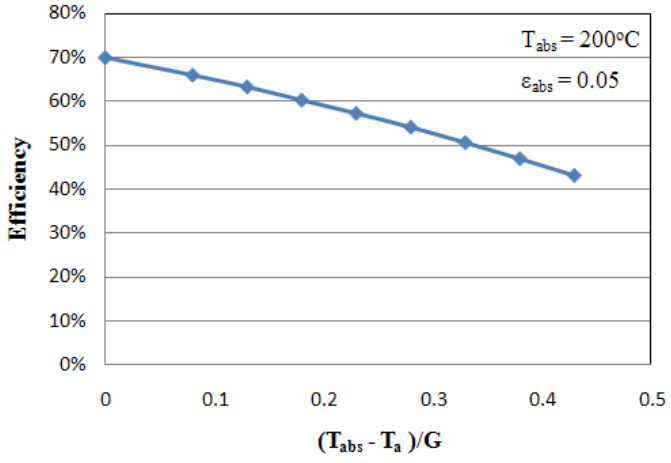


Figure 20: MCT collector efficiency

## CONCLUSION

Preliminary results have been obtained for the performance of a new cavity solar collector incorporating a linear Fresnel micro-concentrator. The performance was numerically simulated using computational fluid dynamics package, ANSYS-CFX. To analyse the thermal performance of the collector, a 2-D numerical simulation of convective and radiation heat loss has been carried out for steady-state laminar conditions and total heat loss coefficient obtained. Natural convection inside the cavity and thermal radiation between surfaces were modeled. The total heat loss over the external boundaries has been studied using different materials for the extruded component supporting the receiver tubes. It was found that to reduce heat loss a low thermal conductivity support component is required. The overall heat loss coefficient of the absorber tube was evaluated (5.8 W/m$^2$K) using CFD simulation. The optical efficiency was determined by ray trace results obtained using the SolTRACE package. Further optical analysis will be carried out to evaluate performance factors such as incidence angle modifiers and shading losses. Finally, the work presented here indicates that the MCT collector has an efficiency of about 60% at its design operating temperature of 200$^o$C.

## ACKNOWLEDGMENTS

The present work is supported by Chromasun Inc., San Jose, CA 95112, USA. The authors would like to thank Mikal Greaves and Andrew Tanner for their support and assistance during the course of this project.

## REFERENCES

1. Juanico, L., 2008, A New design of roof-integrated water solar collector for domestic heating and cooling, *Journal of Solar Energy*, 82, pp. 481-492.
2. Sultana, T., Morrison, G.L, Tanner, A., Greaves, M., Lievre, P.L., and Rosengarten, G., 2010, Heat Loss from Cavity Receiver for Solar Micro-Concentrating Collector, *AuSES Solar Conference*, Canberra, Australia.
3. Petrakis, M., Narakos, G., and Kaplanis, S., 2009, Roof integrated mini-parabolic solar collectors. Comparison between simulation and experimental results, *Open Fuels and Energy Science Journal*, 2, 71-81.
4. Gee, R., Cohen, G., and Greenwood, K., 2003, Operation and preliminary performance of the Duke Solar Power Roof: A Roof-integrated solar cooling and heating system, Duke Solar Energy, LLC, 2101 Westinghouse Boulevard,

Raleigh, NC 27604, *International Solar Energy Conference*, p 295-300.

5. Haberle, A., Berger, M., Luginsland, F., Zahler, C., Baitsch, M., Henning, H., and Rommel, M., 2006, Linear Concentrating Fresnel Collector for Process heat Applications, *Proc. 13th Int. Symp. on Concentrated Solar Power and Chemical Energy Technologies*, Spain.
6. Chromasun, Inc., San Jose, CA 95112, USA, www.chromasun.com
7. Reynolds, D.J., Jance, M.J., Behnia, M., and Morrison, G.L., 2004, An experimental and computational study of the heat loss characteristics of a trapezoidal cavity absorber, *Journal of Solar Energy*, 76, 229-234.
8. ANSYS CFX Help Manual 12.1, www.ansys.com
9. Wang, Y., Dong, X., and Wei, J.H., 2010, Numerical simulation of the heat flux distribution in a solar cavity receiver, *Journal of Frontiers of energy and power engineering in China,Research article*, 1673-7393 *(print).*
10. SolTRACE, Help Manual, National Renewable Energy Laboratory (NREL), www.nrel.gov